MODELING AND CONTROL OF AN ANTI-LOCK BRAKING SYSTEM

Ntsako K. Manyike

School of Electrical & Information Engineering, University of the Witwatersrand, Private Bag 3, 2050, Johannesburg, South Africa

Abstract:

Key words:

1. INTRODUCTION

The technology of vehicles, especially cars all over the world is continously evolving. Along with the many advances in the car manufacturing industry, the safety requirement for cars is of paramount importance. The techniques applied to various cars have already improved system stability and passenger safety with the use of several significant control systems, such as anti-lock braking systems (ABS), active suspension systems, traction control systems etc.

ABS is a system on motor vehicles which prevents the wheel from locking while braking. The purpose of this system is to allow the driver to maintain steering control under heavy breaking and in some situations to shorten braking distance and time. When brakes lock up on wet and slippery roads during a panic stop the driver might lose steering control and the vehicle can spin.

There have been some integrated studies that combined the aforementioned subsystems in order to further enhance vehicle dynamic efficiency. For example, the concept of integrating ABS with active suspension has been introduced and investigated in the work of [**?**]. Many theories and design methods for ABS and active suspension systems have been proposed individually over the years.

2. BACKGROUND

2.1 ABS

It can provide directional stability and shortens the braking distance and time. Various researchers have considered a slip-ratio control of ABS in the use of sliding mode control schemes [3, 4]. A gain-scheduling scheme was proposed for the optimal target-slip tracking of an ABS, where the friction coefficient varied with respect to different vehicle forward speeds [5, 6].

Active suspension systems must be able to guarantee the ride comfort of passengers. Hence, in the design of active suspensions, the improvement of ride quality is a major control objective to be emphasised. In the work of Lin and coworkers [8, 9], a novel nonlinear backstepping [14, 15] control design scheme was developed for both a quarter-car and a half-car active suspension system, which aimed to improve the tradeoff between the ride quality of passenger comfort and the utilisation of suspension travel. In addition, a road-adaptive nonlinear backstepping controller [10] has been applied to the design of a quarter-car active suspension for various road surfaces. The purpose of this paper is to take advantage of ABSs combined with active suspensions to further reduce vehicle braking time and stopping distance. During the braking process, if the vertical normal force is increased (this situation is equivalent to an increase of the weight of a car), the friction force between the car and road surface is increased to help the vehicle to stop in a shorter distance. As normal force cannot be increased naturally, active suspensions should therefore be the tool employed to achieve that adjustment of normal force. With the choice of an appropriate integrated algorithm, the vertical normal force can be adjusted with the braking torque in order to achieve a reduction of braking time and stopping distance.

2.2 Microscope stages

A microscope stage is required to move along all three axes. The vertical motion of the stage provides a focusing mechanism and is usually performed by moving the stage mounting system vertically. The specimen is then moved in the X-Y plane, about the optical centre of the microscope stage, exposing any point of the specimen to the viewer. On the Olympus BX50, this motion is provided by two concentric rotary dials.

Existing automated microscope stages: The automation of microscope stages has been performed by various companies. Geared rotary stepper motors and piezo electric linear motors have been used to provide this linear X-Y motion. Each is suited to a particular application.

The rotary stepper motor solution is the most common solution. They provide micrometer resolution with a relatively compact design and easy control and drive system. Olympus [**?**], Prior Scientific [**?**] and Applied Scientific Instrumentation [**?**] have stages on the market that make use of this technology, for standard microscope applications.

For nanotechnology, the piezo linear motors produced by PI [**?**] are incorporated into an automated stage. The application of a voltage to the piezo-electric crystals causes them to bump the stage along with a resolution of 50 pm and a range of 1 mm. This low range allows for capacitive sensors to provide accurate positional feedback.

Additional options and features offered by these manufacturers include joystick control and RS-232 control. The simplest of systems, suited to the Olympus BX50, range between R40 000 and R50 000 from a local supplier [**?**] or from between R16 000 and R35 000 excluding shipping charges from Prior Scientific, UK [**?**].

2.3 Digital camera systems

The Olympus BX-50 has adopted standard photomicrography camera lenses, namely C- and CS-mounted lenses [**?**]. The capture rate of available digital capture devices range between 1/60 fps, from still cameras, to 30 fps, from video cameras using the National Television Standards Committee (NTSC) system [**?**].

2.4 Linear synchronous motors

LSM's have come into favour because of [**? ?**]:

1. Their accurate positioning capabilities via DC excitation.
2. The lower cost and weight of permanent magnet (PM) movers which do not require power supplies
3. The high thrusts, speeds and efficiencies they can provide.
4. The absence of a transmission which eliminates gearing losses, and increases reliability and dynamic performance.

3. SYSTEM DESIGN

Figure 1 : System Overview

Figure 1 depicts the three sections of the designed system.

3.1 dsPIC30F6014 microcontroller unit

The dsPIC30F6014 MCU [**?**] was used to control the motor. In the case of sinusoidal power signals, it presented digital signals to two digital-to-analog converters (DAC). For the application of PWM power signals, six output-compare channels were used.

3.2 Drive system electronics

Sinusoidal Power Signals: Two 12-bit DAC's produced the A and C phases for both directions. A sequence of inverting summing amplifiers generated the third phase from the redundancy in three-phase systems, and provided bipolar operation. Six Class-AB power amplifiers provided the current necessary to drive the X-Y LSM.

PWM Power Signals: A six channel class-D amplifier provided the current necessary to drive the X-Y LSM through a filter bank. The filter bank was developed to compensate for the armature's low filtering ability.

3.3 X- and Y- direction windings

The armature windings were based on two flat, stacked, orthogonal LSM's as described by Davies [**?**], providing independent two-dimensional movement.

4. STAGE DESIGN

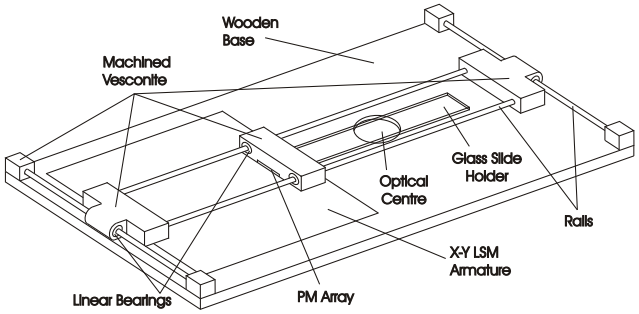

Figure 2 : Stage Design

The stage in *Figure 2* was constructed from a machined wooden base. This material provided the lowest cost and weight when compared to metallic or plastic materials. It hosted the sunken armature which was offset from the optical centre of the stage. It was offset to allow the light to pass through the stage unobstructed, and sunken to allow the railing system to be fitted as low as possible. This provided the closest possible suspension of the PM array, increasing flux linkage. Excessive height also reduces the microscope's focusing range. The railing system consisted of 5 mm diameter silver steel rails on which IKO LBE5 linear bearings were run. The bearings were encased in machined Vesconite, which also served to hold the rails in place, aligned to within 0.01 mm at the ends. A 3 mm thick piece of glass was fitted into the bottom of the central mover, providing a surface on which the specimen could be placed. The cursor PM array was fitted onto the glass, directly below the central mover. This prevented the vertical forces on the PM from generating torques on the central mover's linear bearings, allowing them to move smoothly.

Table 1 : Armature Advantages and Disadvantages

	Advantages	**Disadvantages**
PCB	1) The thin armature reduced leakage flux and eliminated LSM vertical separation. 2) The pole-pitch was exactly matched.	1) 24 series-turns/phase; costly to increase 2) High Cost (R3 000)
Wire-Wound	1) Low Cost (R200) 2) 180 series-turns/phase 3) Well matched pole-pitch	1) Thicker armature increased leakage flux and imposed vertical LSM separation. 2) Timely construction procedure.

4.1 LSM design

The layout specified by Davies [**?**] was scaled for use in this application. The LSM's orthogonal placement provided independent motion along two dimensions because of the associated orthogonal magnetic fields and theoretical zero mutual inductance. The disadvantage of this layout was that the individual LSM's were at different depths from the cursor. The result was that, at the level of the PM array, the lower LSM produced a weaker magnetic field than the upper LSM.

The armature was a slotless design. Although the magnetic field was weaker in this design, the detent forces were eliminated [**?** **?**]. Detent forces are the periodic attractive forces between the PM's and the metallic slots between the windings. In order to achieve smooth motion, these forces must be eliminated.

The LSM was a single sided design, employed to minimise the height of the system. The disadvantage of this design was that less flux was generated [**?**]. A back iron was also neglected because of the associated weight which could not be accommodated by the stage support. This reduced flux linkage.

The topology employed consisted of an active armature and a passive PM cursor [**?**]. The advantage of this topology was that the cursor was electrically isolated from the stage such that no electrical contacts were in motion. This increased durability.

To determine the pole-pitch, the speeds required must be considered. From the Olympus BX50's technical data, the observable fields-of-view range between 0.22 mm and 5.5 mm. From this, and the rate of capture of the digital imaging devices, the linear speeds at which this system can move are between 0.176 mm/s and 44 mm/s. This includes a 20% overlap which allows for accurate digital knitting.

To achieve these low speeds, minimisation of both the pole-pitch and the input frequencies is essential. The relationship between these three variables is given in *Equation 1*. The pole-pitch was limited by the dimensions of available Nd-Fe-B PM's. The smallest available PM's were 8.6 × 8.6 mm × 3 mm, polarised along their shortest dimension. To minimise force-ripple, the ratio of the magnet-length to the machine pole-pitch is 0.8 [**?**]. This ratio results in reduced harmonics in the DC magnetic field and lower thrust, but is essential for smooth motion. Therefore, the system pole-pitch was 10.75 mm and the excitation frequencies needed to be between 0.008 Hz and 2 Hz.

$$v = v_s = 2f\tau \tag{1}$$

where:

v = Linear Velocity (mm/s)
v_s = Synchronous Linear Velocity (mm/s)
f = Input Frequency (Hz)
τ = Pole Pitch (mm)

Two armatures were tested. The first design made use of a PCB. The second was a wire-wound armature. The advantages and disadvantages of both are presented in *Table 1* with a final specification given in *Table 2*. The two PM arrays shown in *Figure 3* were also tested. They represent compromises between size and flux linkage.

Table 2 : Motor Specifications

	Specification	**Value (Units)**
1.	3Φ Connection	Δ
2.	Pole Pairs	6×6
3.	Pole Pitch	10.75×10.75 (mm)
4.	PCB Track Width	0.695 (mm)
5.	PCB Series-Turns/Phase	24×24
6.	Wire-Wound wire ⊘	0.35 (mm)
7.	Wire-Wound Series-Turns/Phase	180×180
8.	Max Current	1.5 (A)
9.	Nd-Fe-B PM Size	8.6×8.6×3 (mm)

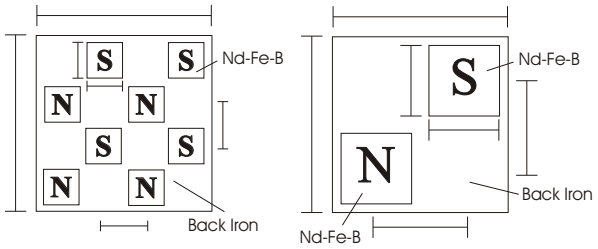

Figure 3 : PM Array Configurations

5. DRIVER SYSTEM

5.1 dsPIC30F6014 microcontroller

The dsPIC MCU was used to generate the six phase signals required to drive both dimensions of the X-Y LSM. The program strategy was designed according to a layered system. The signal generation formed the lowest level of the structure and accepted two inputs, the X- and Y-direction frequencies, called the frequency bus. Subsequent layers existed separately from the generation layer. To control the LSM, a layer asserted a value onto the frequency bus. This provided a means of stacking various layers such as a joystick or RS-232 controller layer.

A 12-bit sampled sinusoid was stored in the program memory using the Page Space Visibility functionality which allowed program memory to be accessed as if it were data memory. The generation layer accepted the two values on the frequency bus and set up timers to interrupt accordingly. On each timer interrupt, the next value for each phase was read from the sinetable using pointers. For sinusoidal power signals, these values were written to the 12-bit dual DAC's using two 12-bit data buses and one 2-bit control bus. For the PWM power signals, these values represented the duty-cycles of the PWM signals and were written into appropriate PWM registers. The PWM signals ran at a chopper frequency of 1.8 kHz. This allowed for 12-bit resolution at the available clock frequency. Open-loop scalar control was implemented. The methodology of the MCU is illustrated in *Figure 4.*

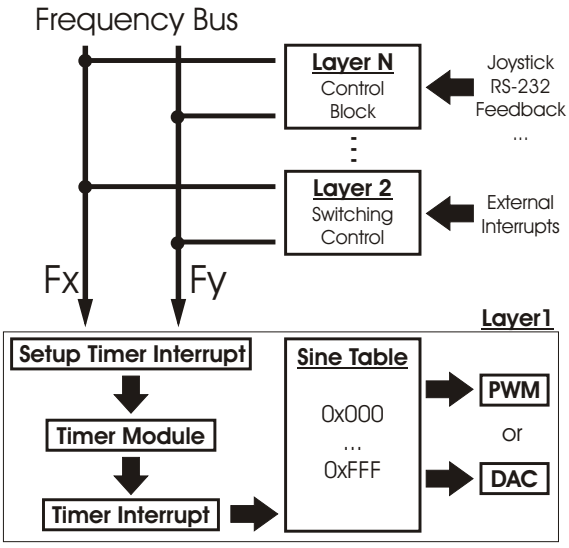

Figure 4 : Controller Methodology

5.2 Drive system electronics

Sinusoidal power signals: The two 12-bit digital buses were connected to two Maxim MX7847BN DAC's. Channel A of the two DAC's produced phases A and C for the X-direction whilst Channel B produced the same for the Y-Direction. Bipolar operation was achieved using inverting, summing, operational amplifier configurations according to the application notes. For each direction, phases A and C were summed in an inverting configuration to produce phase B according to *Equation 2.* Tuning potentiometers were set to within 0.2% fullscale (FS) to achieve phase and amplitude symmetry. The six phase signals formed inputs to the six current gain amplifiers. These were class-AB power amplifier configurations using TIP122 and TIP125 complimentary darlington transistor pairs. They could be driven directly from the TL074 op-amps because of their high current gain ($H_{fe-min} = 1000$). This eliminated excessive external circuitry. A TL074 op-amp was used to ensure accurate amplification by placing the class-AB amplifier in the feedback loop of the op-amp, with a buffered input to the op-amp. The six outputs were connected directly to the X-Y LSM windings.

$$\begin{aligned} i_A + i_B + i_C &= 0 \\ i_B &= -i_A - i_C \end{aligned} \tag{2}$$

PWM power signals: The six TTL logic level PWM signals formed inputs into a six channel class-D amplifier. This consisted of a primary stage in which comparators, made from TL074 op-amps, pushed the voltage signals to the rails. Thereafter, the same TIP122 and TIP125 complimentary darlington transistor pairs were used in an H-bridge configuration to provide current amplification.

It is typically understood that the armature windings filter Voltage Source Inverter PWM signals to produce smoothed current signals. In reality, the -3 dB frequency of the filter created by the armature windings is given by $f = \frac{R}{2\pi L}$. For the designed armatures, the resultant -3 dB frequencies were 3.183 kHz and 17.683 kHz for the wire-wound and PCB armatures respectively. Therefore, the switching frequency permeated through the armatures as current signals with no attenuation. A six channel filter bank was designed to compensate for this effect. Each channel was a second order RLC filter, as shown in *Figure 5.* The resulting -3 dB frequency was 112 Hz.

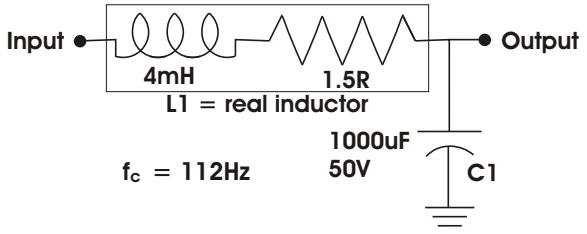

Figure 5 : RLC Filter Circuit

6. RESULTS

Smooth motion was not achieved. The contributing factors are considered below.

6.1 Torsional effects

Motion across the width of the stage was significantly more hap-hazard than that of the movement along the stage's length. The layout and placement of the LSM resulted in the forces being applied at a distance from the linear bearings. The distance at which this force was applied was different for each bearing, resulting in different torques on these bearings. The resultant torsional effect, when combined with frictional variations on each bearing, would mis-align the bearings and cause them to cease. The bearings were released from this state once the cursor had slipped a pole and was pushed backward for a short distance. This effect was due to the offset positioning of the LSM. Not only was this a hindrance to smooth motion, but it was also impractical in terms of it's spacial integration into a microscope system.

6.2 Frictional effects at low speeds

The linear bearings have extremely low frictional coefficients. The static coefficient is, as is typical, higher than the kinetic coefficient. As the magnetic wave built up behind the PM array, the force increased to overcome the static friction. When the force had become substantial enough to overcome this friction, the cursor was thrust forward. Because the frictional coefficient had reduced, the resultant force increased in the direction of movement. The cursor moved suddenly, whilst the magnetic wave did not and thus did not reinforce the original force that was applied to the cursor. Therefore the cursor stopped and was once again affected by static friction. The cycle began again, resulting in periodic motion.

6.3 LSM construction

The layout of the LSM contributed in many ways to the failure to achieve smooth motion. The wire-wound solution produced better results.

PCB armature: The PCB design provided a solution whereby leakage flux was reduced, because of the reduced air-gap associated with a thinner armature relative to the pole-pitch. The differing strengths of the X- and Y-direction windings at the PM level were eliminated because of the alternate layering of X- and Y-windings. This design's major downfall was that, because of construction costs and complexities, only 24 series-turns per phase could be accommodated in the design. In testing, the magnetic field produced could not overcome the inertia of the railing system.

Wire-wound armature: The wire-wound armature produced a strong magnetic field and was able to overcome the inertia of the railing system. A 2.5 mm separation existed between the X- and Y-direction windings because of its construction. The differing strengths of the magnetic fields were evident. This design was able to accommodate 180 series-turns per phase resulting in a 650% increase in efficiency over the PCB design. The system still sourced 2 A from the power supply making it inefficient. The high currents however may be attributed to the extra current needed to overcome the frictional and torsional effects.

Cursor design: The two-magnet design did not offer enough flux linkage to move the cursor successfully. The eight-magnet design worked, but with the obvious spacial consequences. Smooth motion may have been affected by the harmonics in the DC magnetic field.

6.4 Sinusoidal vs. PWM power signals

The natural PWM power signals performed more effectively than the sinusoidal power signals.

Sinusoidal power signals: These signals were highly susceptible to EMI and other sources of noise. The amplification of these signals was inefficient because of the linear electronics involved. The design was flawed by the inability to achieve phase and amplitude symmetry. The finite resolution of 0.2% FS in the tuning circuit resulted in an unbalanced three phase system. When driving the X-Y LSM with this imbalance, high-frequency noise was observed and is analogous to two ocean waves crashing into one another.

PWM power signals: The application of PWM power signals was efficient because the saturated transistors present little resistance in the current path and hence dissipate less energy, requiring smaller heatsinking components. The electronic circuitry was significantly less complex and less susceptible to high frequency noise because of the digital nature of the signals. The use of PWM at the suitably high enough chopper frequency of 1.8 kHz provided a better balanced sinusoidal system after the effective filtering of the filter bank. The chopper frequency was attenuated by 54 dB, in the current waveform, by the filter bank.

7. DISCUSSION

Smooth motion was not achieved since the layout of the X-Y LSM caused torsional effects. The low speeds required by the application caused staggered motion due to the dynamics of the frictional forces in the system. The efficiency was low due to the low 180 series-turns per phase resulting in 2 A being drawn from the power supply. PWM power signals proved more

effective in maintaining phase and amplitude symmetry as opposed to sinusoidal power signals. However, this method required external filter banks ($f_c = 112$ Hz to compensate for the ineffectual filtering ability of the armature. The stacked layout of the X-Y LSM prevented more series-turns from being built into the system, whilst maintaining the low pole-pitch, because it separated the lower windings from the PM array accordingly. The wire-wound armature was a better solution than the PCB design as it could accommodate more series-turns per phase at a lower cost. Therefore, in this layout, the pole-pitch and ampere-turns necessary to provide smooth motion efficiently could not be accommodated.

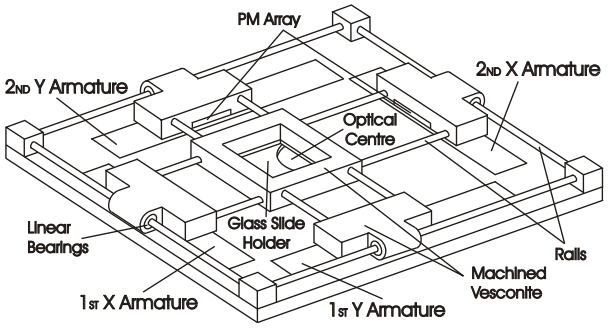

Figure 6 : Recommended Stage

An improved solution is depicted in *Figure 6*, where four individual LSM's are used, two for each dimension. They are placed below the linear bearings, under which the PM array is housed. This prevents any torsional effects from mis-aligning the bearings because adjacent LSM's are excited from the same source. Halbach arrays are recommended to increase flux linkage with the armature, making large PM arrays unnecessary. They will also increase efficiency, accuracy and dynamic response resulting from their sinusoidal magnetic field pattern [**?** **?**]. This new layout also allows the stage to fit centrally about the optical centre, without an offset motor. The railing system is maintained as it helps improve efficiency by reducing friction. A suitable vector control strategy should be implemented to achieve the desired smooth motion. By separating the X- and Y-direction windings, more ampere-turns can be accommodated by building in further depth into each LSM. This is done while maintaining the small pole-pitch, if not reducing it simultaneously, depending on the availability of Nd-Fe-B magnets.

8. CONCLUSION

Slow and smooth motion necessary for the automation of specimen photomicrography could not be achieved due to torsional effects introduced when only two X-Y linear synchronous motors were used to automate an electric microscope stage. To resolve this problem, it is recommended that a layout using four independent linear synchronous motors be implemented.

ACKNOWLEDGEMENT

The author would like to thank Mr. H. Fellows, Mr. A. van Zyl and Mr. S.Q. Davies from the School of Electrical and Information Engineering for their guidance, and Mrs. E. Marais from the Wits Medical School for providing access to the Olympus BX50.

REFERENCES

[1] Public Health Practice Program Office – CDC. "Diagnosis of Tuberculosis Infection and Disease." URL `http://www.phppo.cdc.gov/PHTN/tbmodules/modules1-5/m3/3-m-08.htm`. Last accessed: 1 July 2004.

[2] BIOTEC Laboratories Ltd. "Biotec Products in Development." URL `http://www.biotec.com/fastptb.html`. Last accessed: 1 July 2004.

[3] N. Soh. "Malaria Diagnosis in Just Minutes, Instead of Hours." URL `http://www.ece.nus.edu.sg/events/news/newsarchs.htm`. Last accessed: 1 July 2004.

[4] *Olympus Corporation*. URL `http://www.olympus.com`. Last accessed: 1 July 2004.

[5] *Prior Scientific*. URL `http://www.prior.com`. Last accessed: 1 July 2004.

[6] Applied Scientific Instrumentation. "Multiscan-4 Low Cost Scanning Stage." URL `http://www.asiimaging.com/ms-4.html`. Last accessed: 1 July 2004.

[7] *Physik Instrumente (PI) GmbH & Co.*. URL `http://www.pi.ws`. Last accessed: 1 July 2004.

[8] *Elmulab (Pty) Ltd*. URL `http://www.elmulab.co.za`. Last accessed: 1 July 2004.

[9] H. Ohsaki, H. Xueliang, Y. Tsuboi, and Y. Ootani. "Electromagnetic Characteristics of a coreless surface motor using Halbach permanent magnets." In *4th International Symposium on Linear Drives for Industry Applications*, pp. 105–108. 2003.

[10] S. Inui, M. Naduka, and Y. Ohira. "Experimental Investigation of Thrust of an X-Y LSM." In *3rd International Symposium on Linear Drives for Industry Applications*, pp. 181–185. 2001.

[11] *Microchip Technology Inc*. URL `http://www.microchip.com`. Last accessed: 1 July 2004.

[12] S. Q. Davies. "Design, Construction and Control of a Slot-less X-Y Linear Synchronous Motor." 4th Year Project Report 03P40, School of Electrical and Information Engineering, University of the Witwatersrand, South Africa, 2003.

[13] J. Wang, G. W. Jewell, and D. Howe. "Analysis and Design Optimisation of Slotless Tubular Permanent Magnet Linear Motors." In *3rd International Symposium on Linear Drives for Industry Applications*, pp. 84–89. 2001.

[14] J. F. Gieras and Z. J. Piech. *LINEAR SYNCHRONOUS MOTORS - Transportation and Automation Systems*. CRC Press, 2000.